Identification and validation of autophagy-related genes in hypertrophic cardiomyopathy

RONG-BIN QIU[1,2*], SHI-TAO ZHAO[1,2*], ZHI-WEI LI[3*], RUI-YUAN ZENG[1,2], ZHI-CONG QIU[1,2], HAN-ZHI PENG[1,2], ZHI-QIANG XU [1,2], LIAN-FEN ZHOU[1,2], SONG-QING LAI[1,2] and LI WAN[1,2]

[1]Department of Cardiovascular Surgery, The First Affiliated Hospital, Nanchang University, Nanchang, Jiangxi 330006, P.R. China; [2]Institute of Cardiovascular Surgical Diseases, Jiangxi Academy of Clinical Medical Sciences, The First Affiliated Hospital of Nanchang University, Nanchang, Jiangxi 330006, P.R. China; [3]Department of Cardiothoracic Surgery, Suzhou Kowloon Hospital, Shanghai Jiaotong University School of Medicine, Suzhou, Jiangsu 215028, P.R. China

Received May 23, 2024; Accepted August 16, 2024

DOI: 10.3892/etm.2024.12729

Abstract. Hypertrophic cardiomyopathy (HCM) is an autosomal dominant cardiac disorder characterized by ventricular hypertrophy resulting from the disordered arrangement of myocardial cells, which leads to impaired cardiac function or death. Autophagy (AT) is a biochemical process through which lysosomes degrade and recycle damaged or discarded intracellular components to protect cells against external environmental conditions, such as hypoxia and oxidative stress. AT is closely related to HCM, and thus, serves an important role in myocardial hypertrophy. However, the precise mechanism underlying the regulation of AT in cardiac hypertrophy remains elusive. The present study aimed to examine the role and mechanisms of AT-related genes (ARGs) in HCM through bioinformatics analysis and experimental validation and to identify potential targeted drugs for HCM. In this study, cardiac samples were obtained from healthy individuals and patients with HCM from the GEO database, and screened for differentially expressed ARGs to further investigate their potential interactions and functional pathways. These genes were subjected to functional enrichment analysis to identify potential crosstalk and involved pathways. Based on a protein-protein interaction network, EIF4EBP1, MCL1, PIK3R1, CCND1 and PPARG were identified as potential biomarkers for the diagnosis and treatment of HCM. Furthermore, 10 components with therapeutic potential for HCM were predicted based on the aforementioned hub genes. The results of bioinformatics analysis were validated using H9c2 cells stimulated with angiotensin II, which represented an *in vitro* model of cardiac hypertrophy. Overall, the present study demonstrated that the expression levels of ARGs were substantially altered in HCM. Therefore, these genes may be used as diagnostic biomarkers and therapeutic targets for HCM.

Correspondence to: Professor Li Wan or Dr Song-Qing Lai, Department of Cardiovascular Surgery, The First Affiliated Hospital, Nanchang University, 17 Yongwaizhengjie, Donghu, Nanchang, Jiangxi 330006, P.R. China
E-mail: ndyfy02131@ncu.edu.cn
E-mail: ndyfy03743@ncu.edu.cn

*Contributed equally

Key words: hypertrophic cardiomyopathy, autophagy, biomarkers, database, bioinformatics analysis

Introduction

Hypertrophic cardiomyopathy (HCM) is an autosomal dominant heart disease characterized by asymmetric hypertrophy of the left ventricle, primarily caused by enlarged myocytes, in the absence of other diseases (1,2). The etiology of HCM is mainly associated with genetic factors, endocrine disorders or autoimmune diseases (3). The estimated prevalence of HCM in the general population is ~0.6%, and varies among children, adolescents and adults (4). With advancements in diagnostic techniques, the prevalence of HCM has shown an increasing trend (5). Clinical manifestations of HCM include chest tightness, angina, dyspnea and syncope. These symptoms are progressive and may lead to serious complications such as heart failure and sudden cardiac death (6-8). Despite substantial progress in the treatment of HCM using personalized strategies (9,10), a definitive cure for this condition remains unknown.

Autophagy (AT) is a biochemical process that involves the degradation and recycling of damaged or discarded intracellular components by lysosomes to protect cells against external environmental conditions, such as hypoxia and oxidative stress (11). Administration of AT inducers, such as rapamycin, in animal models, inhibits mTOR and promotes AT, effectively protecting cardiomyocytes and improving cardiomyopathy phenotypes (12,13). In addition, studies have demonstrated a close relationship between AT and HCM, suggesting that targeting AT is a promising therapeutic strategy for HCM (14-16). However, the precise roles of AT-related genes (ARGs) in HCM remain unclear, necessitating further investigation of the relationship between ARGs and HCM.

In this study, key ARGs related to the development of HCM were identified using bioinformatics analysis. The association between these genes and HCM was determined through functional annotation, pathway enrichment, protein-protein interaction (PPI) and immune infiltration analyses. In addition, potential drugs for the treatment of HCM were predicted, and the results of bioinformatics analysis were validated through reverse transcription-quantitative PCR (RT-qPCR). The findings provide a valuable theoretical foundation for the development of novel diagnostic and therapeutic strategies for HCM.

Materials and methods

Data collection and processing. The HCM dataset GSE180313 (17) was obtained from the Gene Expression Omnibus (GEO) database (https://www.ncbi.nlm.nih.gov/geo/). This dataset contains heart tissues from 7 healthy individuals and 13 patients with HCM. Preprocessed and merged data were integrated into a unified dataset. The 'limma' package (18) in R software (v.3.6.3) (19) was used to identify differentially expressed genes (DEGs) between the HCM and control groups, with the screening criteria being set as a $|\log_2 FC|$ value of <0.5 and a P-value of <0.05. The 'ggplot2' package (20) in R was used to generate heat maps and volcano plots. Information regarding ARGs was obtained from the Human Autophagy Database (http://www.autophagy.lu/index.html) and the Gene Set Enrichment Analysis (GSEA) website (http://software.broadinstitute.org/gsea/index.jsp). The extracted ARGs were processed and integrated into a gene set known as ARGs. GSEA was used to investigate the overall association between AT and HCM and identify potential biological processes involving ARGs that were associated with the pathogenesis of HCM. Genes in the GSE180313 dataset were scored using the AT dataset from GSEA, resulting in the calculation of normalized enrichment scores (NESs). P<0.05 was considered to indicate significant enrichment. The workflow of the present study is shown in Fig. S1.

Identification and functional enrichment analysis of differentially expressed ARGs (DEARGs). DEARGs were obtained by intersecting the DEGs identified in the GSE180313 dataset with the integrated ARG set. The overlapping genes (DEARGs) were visualized on a Venn diagram. Subsequently, the cluster profiler package (v4.8.3) (21) in R and DAVID (david.ncifcrf.gov/) were used to implement Gene Ontology (GO; https://geneontology.org/) and Kyoto Encyclopedia of Genes and Genomes (KEGG; https://www.genome.jp/kegg/) enrichment analyses of DEARGs. P<0.05 was considered to indicate significant enrichment.

PPI network and identification of hub genes and key modules. DEARGs were imported into the Search Tool for the Retrieval of Interacting Genes/Proteins (STRING) database (v11.09) (https://string-db.org/) for PPI analysis with default settings. The resulting PPI network was visualized using Cytoscape software (v.3.7.2) (22). Subsequently, the MCODE plug-in (V 3.7.1) (20) was used to filter and visualize key PPI networks, resulting in the identification of key modules containing hub genes.

Receiver operating characteristic (ROC) analysis of hub genes. The ROC curves of hub genes were constructed using data from the GSE180313 and GSE36961 (23) datasets. The area under the curve (AUC) was quantified for comparison, and only genes with AUC values of >0.6 were considered to have statistically significant diagnostic potential.

Immune infiltration analysis. To investigate the immune microenvironment of HCM and key DEARGs, CIBERSORTx (https://cibersortx.stanford.edu/) was employed to analyze the differences in immune infiltration between patients with HCM and healthy controls. Additionally, this algorithm was utilized to determine the proportions of various immune cell types.

Prediction of therapeutic drugs. Key differentially expressed AT-associated genes and compound interaction data from the Drug Signatures Database (DSigDB; http:/dsigdb.tanlab.org/) were extracted using the Enrichr online tool (http:/amp.pharm.mssm.edu/Enrichr). Drugs for the treatment of HCM were predicted based on hub genes.

Cell culture and model construction. The H9c2 immortalized rat cardiomyocyte-like cell line (The Cell Bank of Type Culture Collection of The Chinese Academy of Sciences) is commonly used in cardiac research *in vitro* (24). H9c2 cells were cultured in high-glucose DMEM (Hyclone; Cytiva) supplemented with 10% fresh fetal bovine serum (HyClone; Cytiva) and 1% penicillin-streptomycin (Gibco; Thermo Fisher Scientific, Inc.) under standard conditions (37˚C, 5% CO_2, 95% humidity and 21% oxygen). Cells from passages 3-10 were used for subsequent experiments. Angiotensin II (AngII; GlpBio Technology, Inc.) was used to induce hypertrophy in H9c2 cells. The cells were incubated with AngII at different concentrations (50, 100, 200 and 400 nM) at 37˚C for 24 h, and the optimal concentration was determined based on the mRNA and protein expression of atrial natriuretic peptide (ANP) and brain natriuretic peptide (BNP). For further experimentation, the cells were incubated with the determined optimal concentration of AngII at 37˚C for 12, 24, 36 and 48 h.

RT-qPCR. Total RNA was extracted from H9c2 cells using TRIzol reagent (Beijing Solarbio Science & Technology Co., Ltd.) and reverse transcribed using the PrimeScript RT reagent kit (Monad Biotech Co., Ltd.) according to the manufacturer's instructions. qPCR was conducted using the SYBR Green qPCR Master Mix (cat. no. B21203; Bimake.com) on a BIO-RAD CFX Connect Real-Time PCR Detection System (Bio-Rad Laboratories, Inc.). The qPCR protocol included an initial denaturation step at 95˚C for 10 min, followed by 40 cycles of thermal cycling with denaturation at 95˚C for 15 sec and annealing at 60˚C for 1 min. The primer sequences used for qPCR are shown in Table SI. ACTB served as the internal reference, and the relative mRNA expression of target genes was calculated using the Cq ($2^{-\Delta\Delta Cq}$) method (25).

Western blotting. To extract total proteins, H9c2 cells were lysed in RIPA buffer supplemented with protease inhibitors (Beijing Solarbio Science & Technology Co., Ltd.) on ice. The extracted proteins were quantified using a BCA assay kit (GlpBio Technology, Inc.) and denatured by boiling for

5 min, and subsequently separated by on 12% gels by sodium dodecyl sulfate-polyacrylamide gel electrophoresis, with 40 μg of protein loaded per lane. The separated proteins were transferred to a PVDF membrane (MilliporeSigma), which was incubated with 5% skimmed milk powder at room temperature for 2 h on a shaker. Subsequently, the membrane was incubated with primary antibodies against ANP (1:500; cat. no. 27426-1-AP; Proteintech Group, Inc.), BNP (1:500; cat. no. A2179; ABclonal, Inc.), LC3 (1:1,000; cat.no. 381544; Chengdu Zen-Bioscience Co., Ltd.), P62 (1:1,000; cat. no. 380612; Chengdu Zen-Bioscience Co., Ltd.) and β-actin (1:1,000; cat. no. 66009-1-Ig; Proteintech Group, Inc.) at 4˚C overnight. The following day, the membrane was incubated with horseradish peroxidase-conjugated mouse and rabbit secondary antibodies (1:5,000; cat. nos. 511103 and 511203, respectively; Chengdu Zen-Bioscience, Co., Ltd.) at room temperature for 2 h. Protein bands were visualized using the Ultra High Sensitivity ECL kit (catalog no. GK10008; GlpBio Technology, Inc.) and captured using the FluorChem FC3 System (ProteinSimple). ImageJ software (v1.8.0.345; National Institutes of Health) was used to semi-quantify the optical density of protein bands.

Detection of autolysosome acidification. To assess the level of AT in cells, LysoTracker Red was used to label intracellular lysosomes, as autophagosomes can bind to lysosomes. Briefly, H9c2 cells were incubated with 50 nM LysoTracker Red working solution (Beyotime Institute of Biotechnology) at 37˚C for 30 min in the dark and subsequently examined using a fluorescence microscope.

Immunofluorescence analysis. LC3 expression in H9c2 cells was detected through immunofluorescence staining. Briefly, the cells were washed twice with PBS, fixed with 4% paraformaldehyde (biosharp life sciences) at room temperature for 10 min, blocked with 2% BSA (cat. no. CAS#9048-46-8; Shanghai Yuanye Bio-Technology Co., Ltd.) at room temperature for 30 min and incubated with anti-LC3 antibody (1:200; cat. no. 381544; Chengdu Zen-Bioscience Co., Ltd.) at 4˚C overnight. The following day, the cells were incubated with a fluorescently labeled secondary antibody (1:200; cat. no. A32732; Thermo Fisher Scientific, Inc.) at room temperature for 1 h. Thereafter, nuclei were stained with DAPI at room temperature for 5 min and the cells were examined using a fluorescence microscope.

Statistical analysis. Statistical analysis was performed using the GraphPad Prism 8 software (Dotmatics). The unpaired two-tailed Student's t-test was used to compare the differences between two groups. One-way analysis of variance and Dunnett's multiple comparison test were employed to assess the differences among multiple groups. Data are expressed as the mean ± standard deviation of 3 repeats. $P<0.05$ was considered to indicate a statistically significant difference.

Results

Study protocol. The overall protocol of the present study is shown in Fig. S1. The patient data used in the present study were derived from the GSE180313 dataset in the GEO database.

Identification of DEGs between the HCM and control groups. After pre-processing and normalization of the GSE180313 dataset, a total of 966 DEGs were identified between the HCM and control groups. Of these 966 DEGs, 510 genes were upregulated and 456 genes were downregulated. A volcano plot and a heat map were generated to visualize the DEGs (Fig. 1A and B).

Identification of DEARGs and enrichment analysis. GSEA was used to compare ARGs between the HCM and control groups. Fig. 1C demonstrates the significant differences in ARG expression between the two groups ($|NES|=1.521$; $P<0.05$). This indicates that ARGs could be a crucial characteristic of HCM and that their dysregulation supports a link between HCM and autophagy. Furthermore, a total of 1,167 ARGs were identified after pre-processing of the integrated gene set. These ARGs were intersected with DEGs to obtain 58 DEARGs (Fig. 1D). A heat map was generated to visualize the expression patterns of these DEARGs in the HCM and control groups (Fig. 1E).

Functional and mechanistic analyses of DEARGs. To investigate the functions and pathways of DEARGs, GO and KEGG enrichment analyses were performed using DAVID. The results demonstrated that DEARGs were significantly enriched in biological processes such as 'peptidyl-serine phosphorylation', 'cellular response to oxidative stress', 'regulation of autophagy' and 'response to UV'; molecular functions such as 'protein serine kinase activity', 'tau protein binding' and 'death domain binding'; and cellular components such as the 'mitochondrial outer membrane' and 'organelle outer membrane' (Fig. 2A-C). KEGG analysis demonstrated that the DEARGs were notably enriched in the 'AGE-RAGE signaling pathway in diabetic complications', 'PI3K-Akt signaling pathway', 'measles', 'hepatitis C', 'AMPK signaling pathway' and 'EGFR tyrosine kinase inhibitor resistance' (Fig. 2D). Interactions were identified between DEARGs and the aforementioned functions and pathways through gene and pathway cross-talk mapping, suggesting that multiple genes and pathways may be involved in the regulation of DEARGs in HCM (Fig. 2E-H). Overall, these findings suggested that ARGs regulate the progression of HCM through intricate interplay among multiple gene functions and pathways.

PPI network analysis, functional module construction and hub gene identification. A PPI network of 58 DEARGs was constructed using the STRING database (Fig. 3A). After the network was imported into the Cytoscape software, the Maximal Clique Centrality algorithm was used to identify a sub-network comprising 32 hub genes. To filter these hub genes, the MCODE plug-in was used to identify important functional modules within the PPI network. Notably, a key cluster in the network consisted of a functional module with 10 nodes and 14 edges, including EIF4EBP1, MCL1, PIK3R1, CCND1, PPARG, SMPD1, RICTOR, NOS3, SNCA and UBB. Fig. 3B and C illustrate the interactions between DEARGs and hub genes.

Diagnostic value of the hub genes. ROC curves were generated to evaluate the diagnostic efficacy of the 10 hub genes (Fig. 4A). In the GSE180313 dataset, all hub genes exhibited AUC values

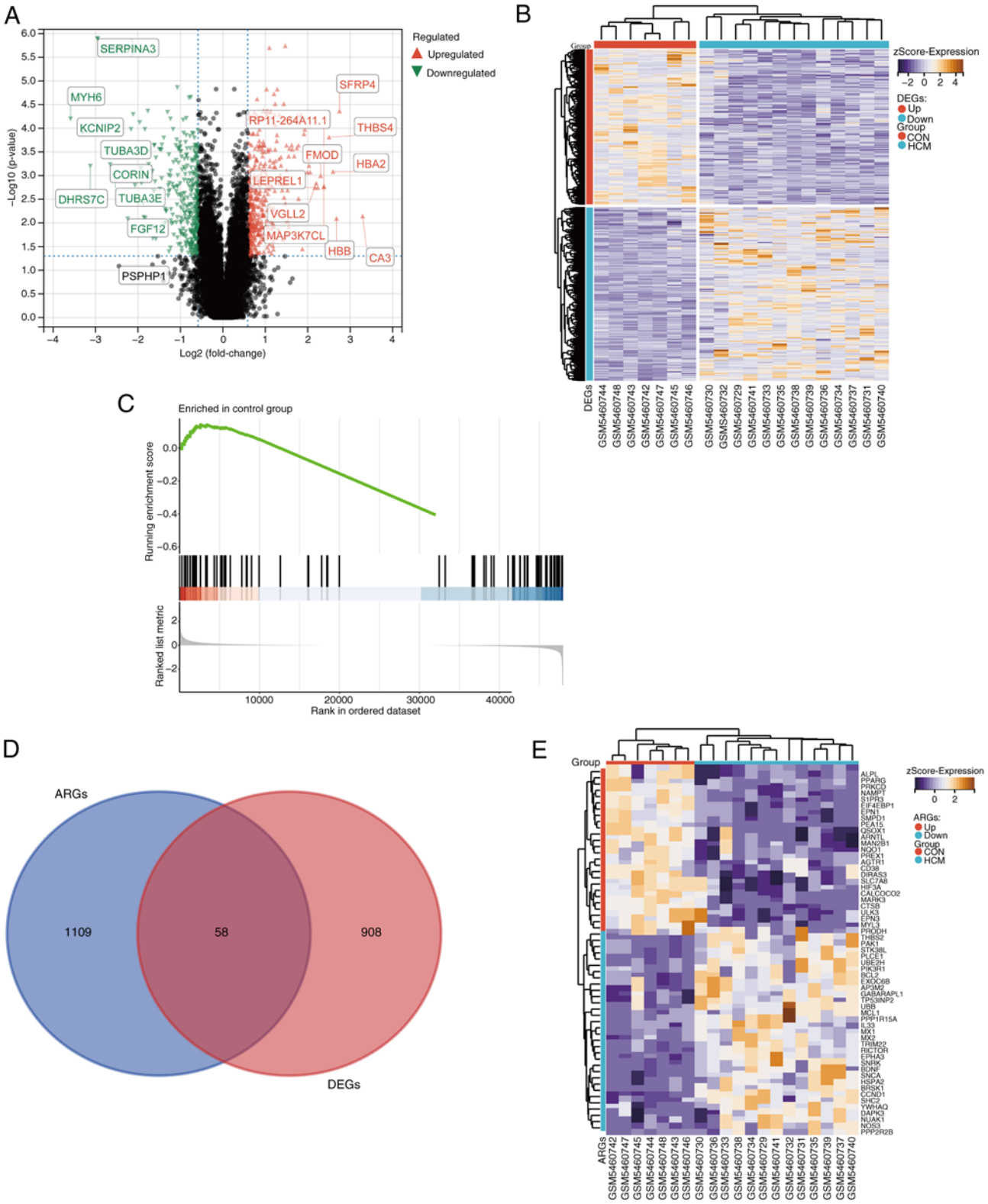

Figure 1. Identification of DEGs in hypertrophic cardiomyopathy. (A) Volcano plot of DEGs in the GSE180313 dataset (log_2FC >0.5 and adjusted P<0.05). (B) Heatmap clustering of genes with markedly different expression in HCM compared with normal control samples in GSE180313 (log_2FC >0.5 and adjusted P<0.05). (C) Gene Set Enrichment Analysis of ARGs in the GSE180313 dataset. (D) Venn diagram showing common genes between the GSE180313 dataset and ARGs. (E) Clustered heatmap of differentially expressed ARGs in the GSE180313 dataset. Correlation coefficients are plotted with negative correlation shown in purple and positive correlation shown in orange. ARG, autophagy-related gene; CON, control; DEG, differentially expressed gene; FC, fold change; HCM, hypertrophic cardiomyopathy.

of >0.8, indicating a significant association with HCM and promising diagnostic potential. An external dataset (GSE36961) was used to validate these findings (Fig. 4B). Notably, discrepancies were observed in the results of hub gene analysis between the two datasets. During the validation of external datasets, it was observed that the AUC values for EIF4EBP1,

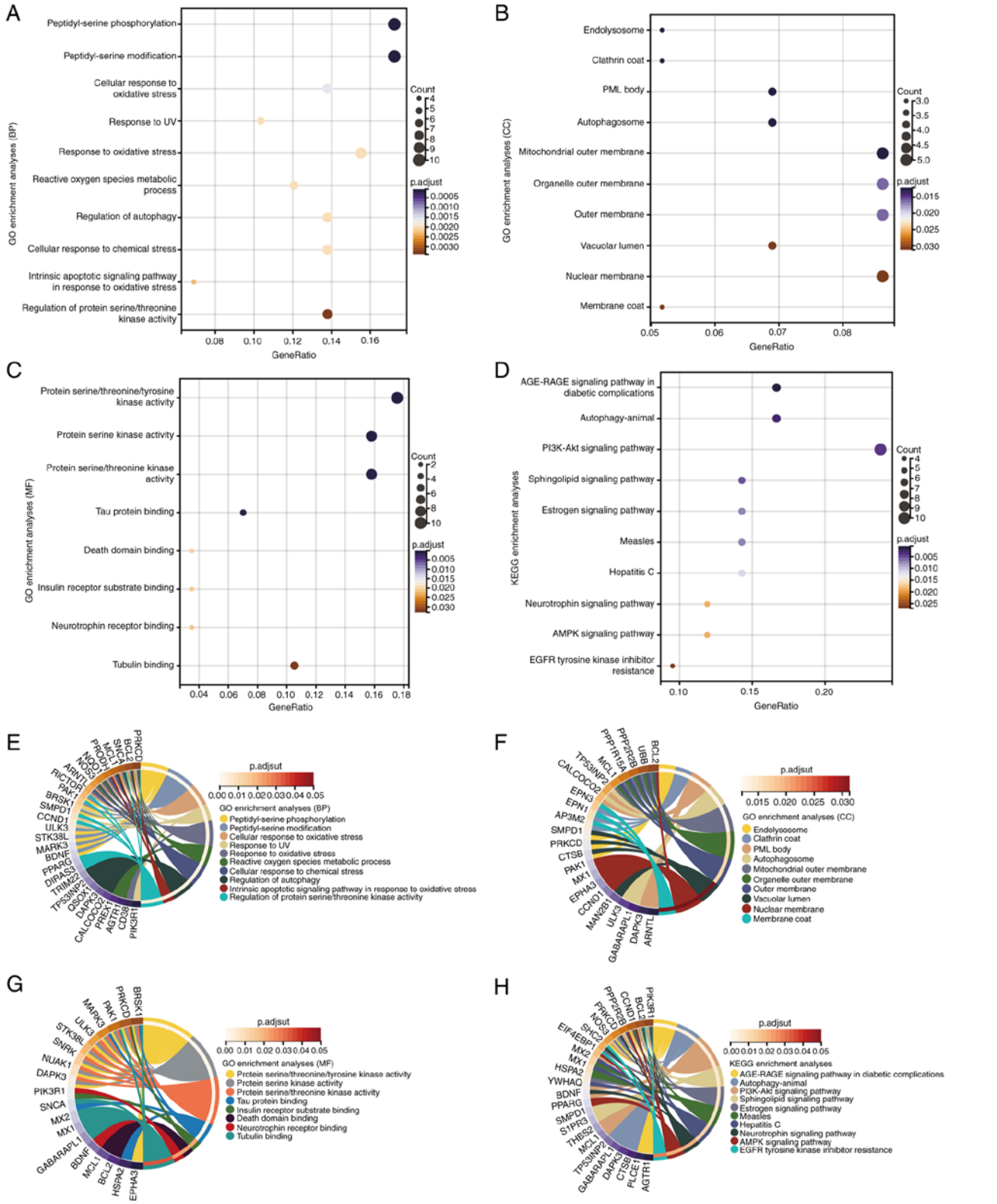

Figure 2. GO and KEGG enrichment analyses of DEARGs. GO enrichment analysis of DEARGs in the (A) BP, (B) CC and (C) MF categories. (D) KEGG enrichment analysis of DEARGs. Crosstalk analysis between DEARGs and gene functions in (E) BP, (F) CC and (G) MF categories, and (H) KEGG pathways. AGE-RAGE, advanced glycation end product-receptor for advanced glycation endproducts; AMPK, AMP-activated protein kinase; BP, biological process; CC, cellular component; DEARG, differentially expressed autophagy-related gene; GO, Gene Ontology; KEGG, Kyoto Encyclopedia of Genes and Genomes; MF, molecular function; p.adjust, adjusted P-value; PML, promyelocytic leukemia.

MCL1, and SMPD1 were <0.7, indicating that these three hub genes exhibit limited diagnostic performance for HCM. By contrast, most other hub genes demonstrated robust diagnostic capabilities (AUC >0.7), suggesting a potential association between autophagy and HCM. Nonetheless, the significance of these hub genes warrants further investigation in future studies

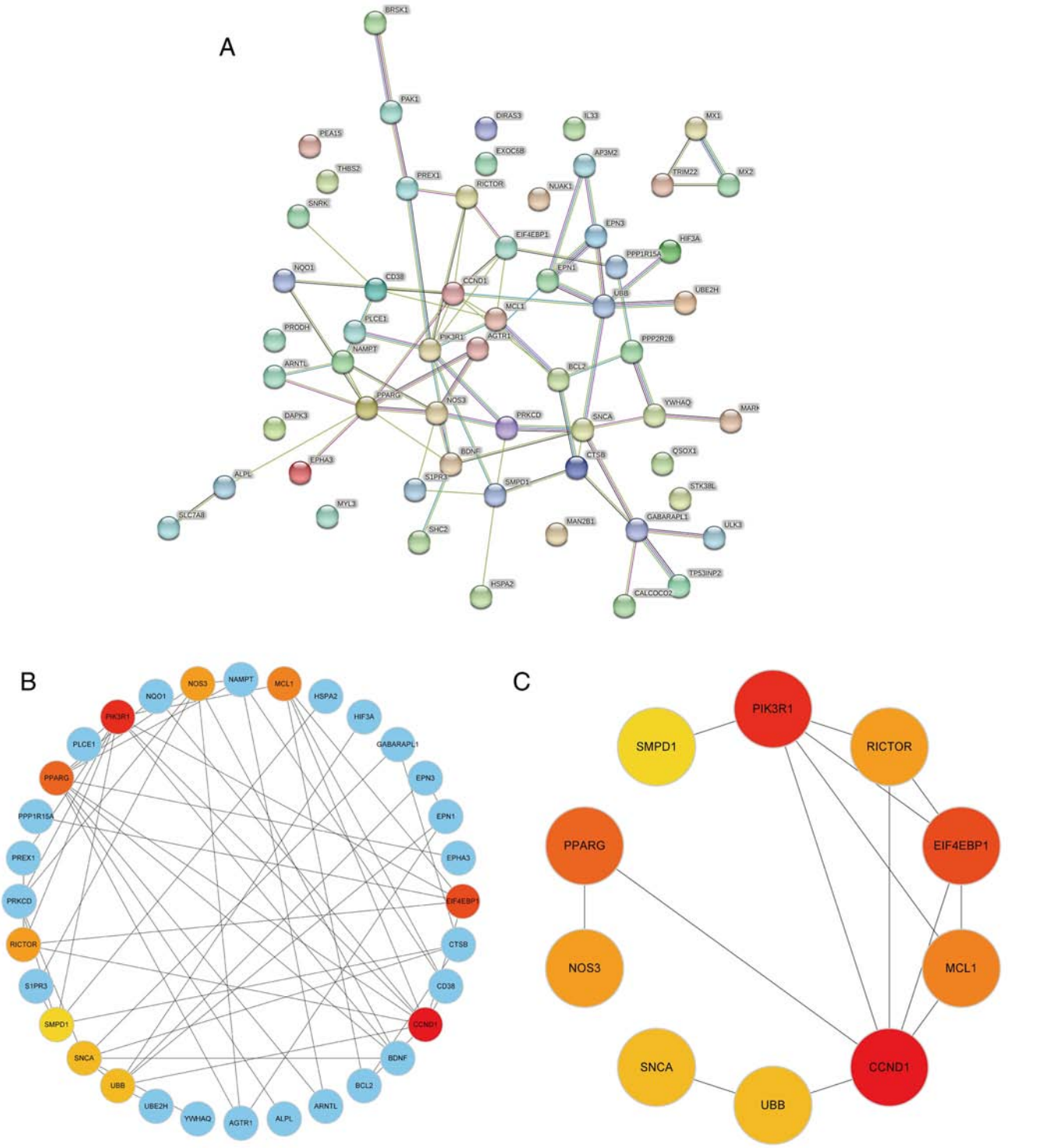

Figure 3. PPI network and identification of hub genes. (A) PPI network of DEARGs constructed using the Search Tool for the Retrieval of Interacting Genes/Proteins database. (B) Crosstalk between the top 10 hub genes based on the Maximal Clique Centrality algorithm and other DEARGs. (C) Crosstalk among the 10 hub genes, where the intensity of the dot color represents the higher rank of the hub gene. DEARG, differentially expressed autophagy-related gene; PPI, protein-protein interaction.

Prediction of drugs and molecular docking simulations. The DSigDB in the Enrichr platform was used to identify small-molecule drugs targeting hub genes for the treatment of HCM. A total of 1,332 drugs with potential therapeutic value were identified based on the degree of gene-compound match and median number, with the screening criteria being set as a false discovery rate of <0.05 and composite scores of >5,000. The top 10 small-molecule drugs with the most significant impact on the expression of hub genes are shown in Fig. 5A. Among these, rapamycin and melatonin are the top two candidates. Fig. 5B and C show the molecular structure of rapamycin and melatonin (Mel; N-acetyl-5-methoxytryptamine). Research has demonstrated that rapamycin exerts a notable effect on the treatment and prevention of HCM (26,27). Mel

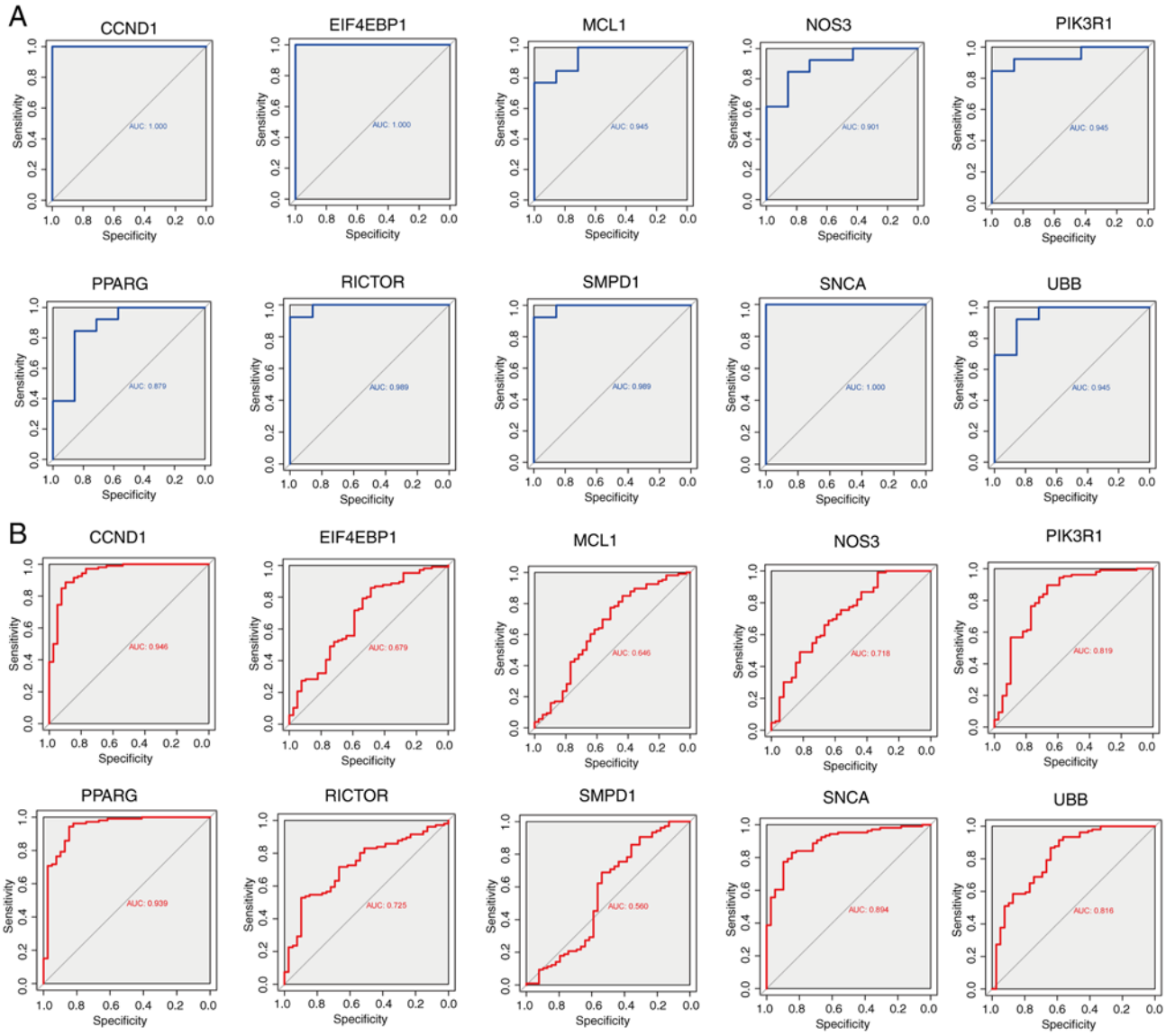

Figure 4. Assessing the diagnostic value of hub genes. (A) ROC curves showing the diagnostic capability of hub genes for HCM in the GSE180313 dataset. (B) ROC curves showing the diagnostic capability of hub genes for HCM in the GSE36961 dataset. AUC, area under the curve; HCM, hypertrophic cardiomyopathy; ROC, receiver operating characteristic.

possesses antioxidant properties and exerts protective effects against various cardiovascular diseases, including diabetic cardiomyopathy and myocardial hypertrophy (28,29). To gain insights into the binding between hub genes and predicted drugs, molecular docking simulations were performed using rapamycin and Mel as examples (Fig. 5D and E).

Relationship between ARGs and immune cell infiltration in HCM. Cellular and humoral immune functions serve a crucial role in the development of HCM (30). The relative proportions of infiltrating immune cells in heart samples from the GSE180313 dataset were assessed and quantified using the CIBERSORT algorithm (Fig. 6A). The resulting heatmap illustrates the relationships between various infiltrating immune cells (Fig. 6B). In addition, violin plots were generated to visualize the expression profiles of the 20 immune cell subtypes in the control and HCM groups (Fig. 6C). Only the infiltration levels of T follicular helper (Tfh) cells were significantly different between the HCM and control groups, with lower levels being observed in the HCM group. Therefore, Tfh cells were identified as differentially infiltrating immune cells. Furthermore, the correlation between immune cells and the 10 hub DEARGs was examined (Fig. 7). Nine hub genes, except for CCND1, exhibited varying correlations with six types of immune cells, namely Tfh cells, monocytes, neutrophils, regulatory T cells, resting natural killer cells and T cells CD4 memory resting. These findings suggested that the hub genes serve an important role in the immune response to HCM.

Validation of hub genes in an in vitro model of HCM. To validate the expression of the hub genes EIF4EBP1, MCL1, PIK3R1, CCND1, PPARG, SMPD1, RICTOR, NOS3, SNCA and UBB *in vitro*, H9c2 cells were stimulated with AngII to induce HCM. Western blotting and RT-qPCR were used to determine the optimal concentration and duration of AngII treatment. The results demonstrated that when H9C2 cells

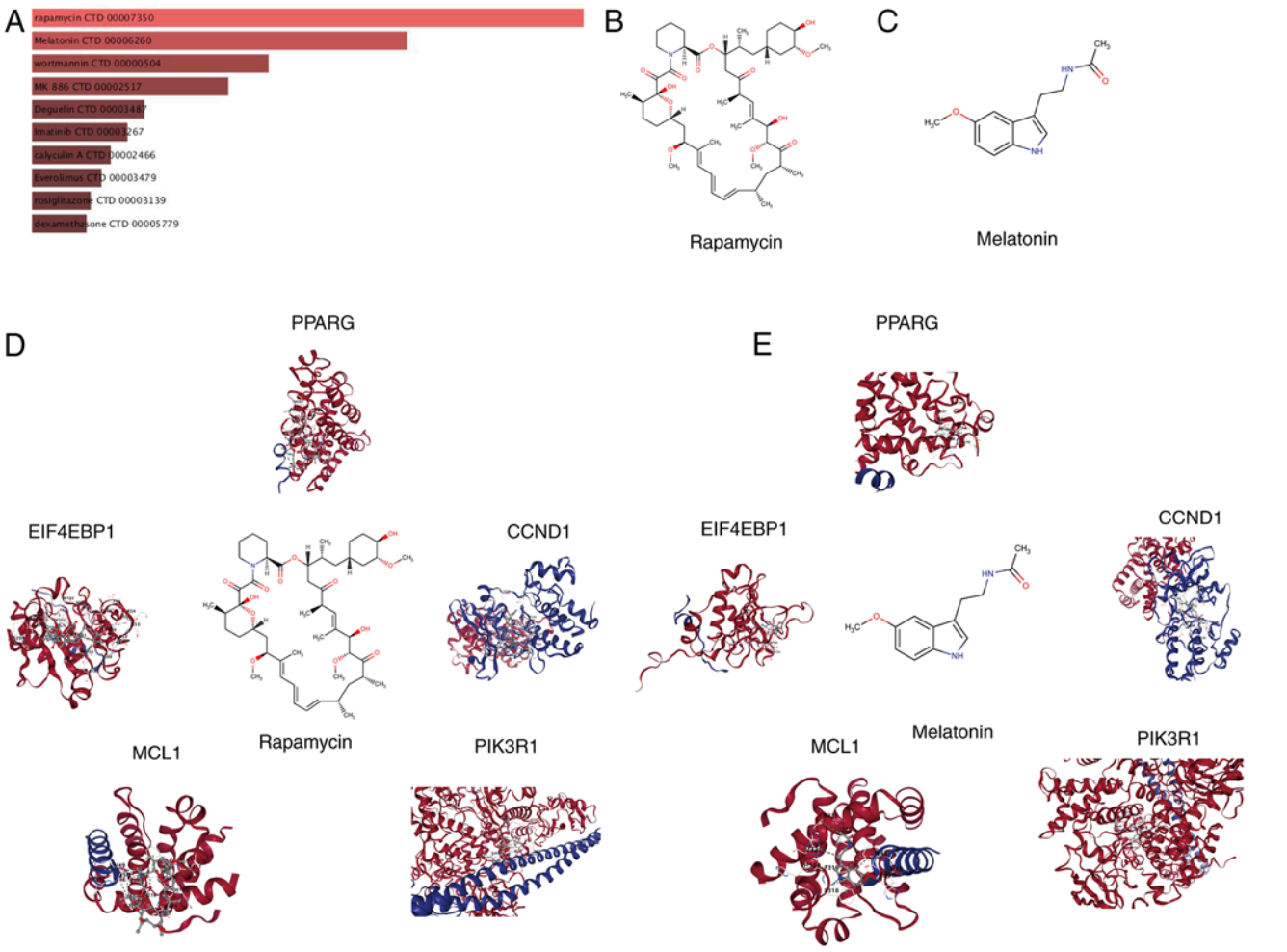

Figure 5. Potential target drug prediction and molecular docking simulation. (A) Top 10 targeted drugs predicted and ranked based on their combined score in the Drug Signatures Database. (B) Chemical structure of rapamycin. (C) Chemical structure of melatonin. The molecular docking simulation revealed the formation of a stable complex between (D) rapamycin and (E) melatonin and hub genes.

were pretreated with AngII for the same duration, the highest protein expression levels of ANP and BNP were observed in the 100 nM AngII group (Fig. 8A-C). Additionally, when H9C2 cells were pretreated with 100 nM AngII for different time periods, the highest ANP and BNP protein expression levels were found at 24 h of pretreatment (Fig. 8D-F). Consistent with these changes in protein expression, the mRNA levels also corroborated this finding (Fig. 8G-J). Therefore, a pretreatment of H9C2 cells with 100 nM AngII for 24 h was selected to induce hypertrophy. Western blotting was used to evaluate the expression levels of the AT-associated proteins LC3 and P62 in the AngII and control groups (Fig. 9A). As shown in Fig. 9B and C, the LC3/β-actin ratio was significantly lower and the protein expression of P62 was higher in the AngII group. Furthermore, autolysosome acidification was detected, and immunofluorescence analysis was performed to assess the level of AT. H9c2 cells stained with LysoTracker Red showed reduced fluorescence intensity in the AngII group compared with that in the control group (Fig. 9D). Immunofluorescence analysis revealed a decrease in LC3 fluorescence intensity in the AngII group compared with that in the control group (Fig. 9F). The aforementioned results indicate that autophagy is reduced in the AngII-induced H9C2 cell hypertrophy model. To ensure the reliability of the results, RT-qPCR was performed to evaluate the expression levels of hub genes in both groups. Based on PPI network analysis, EIF4EBP1, MCL1, PIK3R1, CCND1 and PPARG were identified as the most significant hub ARGs associated with HCM. RT-qPCR revealed that EIF4EBP1 and PPARG were downregulated, while MCL1, PIK3R1 and CCND1 were upregulated after treatment with AngII (Fig. 10). Therefore, we propose that EIF4EBP1, MCL1, PIK3R1, CCND1 and PPARG play roles in the regulation of autophagy in HCM.

Discussion

HCM is a prevalent hereditary cardiac disease that predisposes individuals, especially young athletes, to sudden death, also known as exercise-induced sudden cardiac death (31,32). Although HCM does not progress rapidly, its complications such as sudden arrhythmogenic death, heart failure and atrial fibrillation can occur abruptly or worsen under any circumstances, posing a severe threat to the life of patients (33). According to the 2018 Epidemiological Survey statistics, HCM remains a major health concern worldwide, affecting ~88% of the global population and imposing a long-lasting

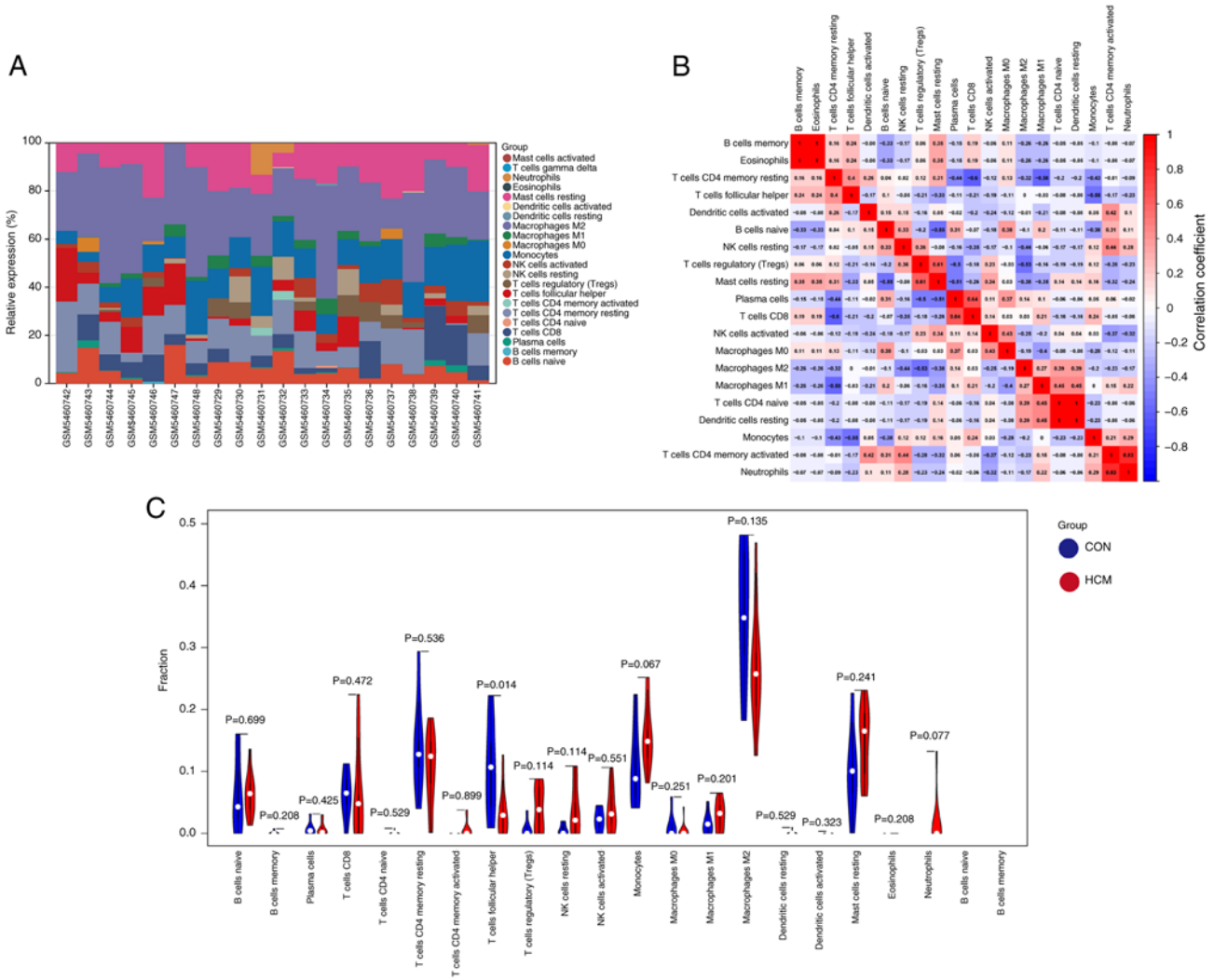

Figure 6. Association between SRGs and immune cell infiltration in HCM. (A) Proportion of infiltrating immune cells in the samples from the GSE180313 dataset based on the CIBERSORT algorithm. (B) Correlation heatmap of DIICs in the GSE180313 dataset displaying the correlation coefficients, with negative correlations represented by blue and positive correlations represented by red. (C) Violin plots showing the comparison of infiltrating immune cells between normal and hypertrophic cardiomyopathy samples in the GSE180313 dataset. DIICs, differentially infiltrating immune cells; NK, natural killer.

socioeconomic burden (34). However, no precise and efficient therapeutic strategy has been developed to date. AT serves an essential role in the development and progression of cardiovascular diseases such as myocardial infarction, aortic coarctation, atherosclerosis and ischemic cardiomyopathy (35-37). Therefore, targeting AT represents a promising strategy for the treatment of HCM. However, the precise role of AT in the pathogenesis of HCM warrants further investigation. In the present study, bioinformatics analysis was used to examine the roles and mechanisms of ARGs in the development of HCM to explore novel avenues for effective treatment.

A total of 58 DEARGs associated with HCM were identified through comprehensive analysis of a GEO dataset and an ARG set. GSEA revealed a significant association between ARGs and HCM, suggesting that AT serves a crucial role in the development of HCM. Furthermore, GO functional annotation and KEGG pathway enrichment analysis demonstrated that the DEARGs were closely associated with various biological processes, cellular components and molecular functions related to AT (Fig. 2). Notably, the findings indicated that the pathogenesis of HCM involves not only AT but also other classical pathways such as the 'AGE-RAGE signaling pathway in diabetic complications' and the 'PI3K-Akt signaling pathway'. AT serves as a cytoprotective mechanism that maintains cellular homeostasis by regulating intracellular and extracellular catabolic and anabolic processes through the lysosomal degradation pathway (38,39). Alterations in the levels of cardiomyocyte AT have been reported to induce functional or morphological changes, including apoptosis, atrophy, fibrosis or hypertrophy (40-42). A recent study revealed that excessive cardiomyocyte AT can result in lysosomal storage disorders that lead to cellular damage and cardiac dysfunction (16). These findings highlight the extensive investigation of the role of AT in HCM, while emphasizing the need for further exploration of other molecules and pathways. In the present study, PPI network analysis revealed 10 hub genes (EIF4EBP1, MCL1, PIK3R1, CCND1, PPARG, SMPD1, RICTOR, NOS3, SNCA and UBB) associated with the development of HCM. The diagnostic value of these hub genes was assessed through ROC analysis and validated through cellular experiments. All hub genes except for SMPD1 exhibited significant diagnostic potential. Notably, EIF4EBP1, MCL1, PIK3R1, CCND1 and

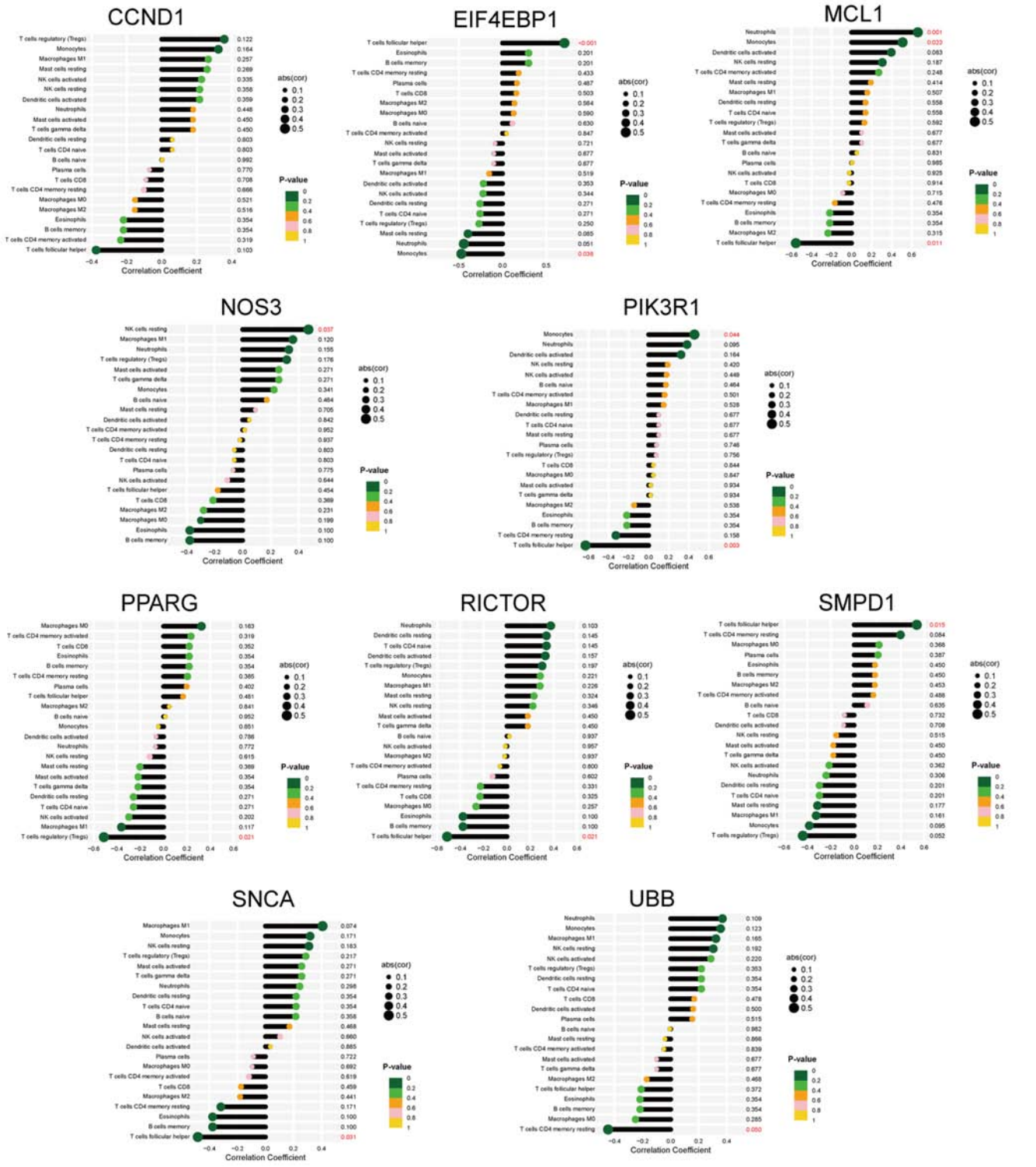

Figure 7. Correlation between key genes and infiltrating immune cells. The association between hub genes and immune cell infiltration is presented, only including immune cells with a P-value <0.05. abs(cor), absolute value of correlation; NK, natural killer.

PPARG were differentially expressed between control and AngII-treated H9c2 cells. In particular, PIK3R1, MCL-1 and CCND1 were significantly upregulated in AngII-treated cells. These results suggested that the aforementioned five ARGs serve as promising therapeutic targets for HCM.

EIF4EBP1 functions as a regulatory protein in cell signaling pathways and is involved in the initiation and progression of various diseases (43-46). Upregulation of EIF4EBP1 has been shown to delay the progression of systemic lupus erythematosus through B-cell AT (43). Additionally, EIF4EBP1 acts as a tumor suppressor gene. Upregulation of EIF4EBP1 promotes the development and metastasis of breast cancer, whereas downregulation of EIF4EBP1 in breast cancer impedes the proliferation of pituitary tumor cells (45,46). Several studies have indicated that EIF4EBP1 serves as a biomarker for evaluating the prognosis

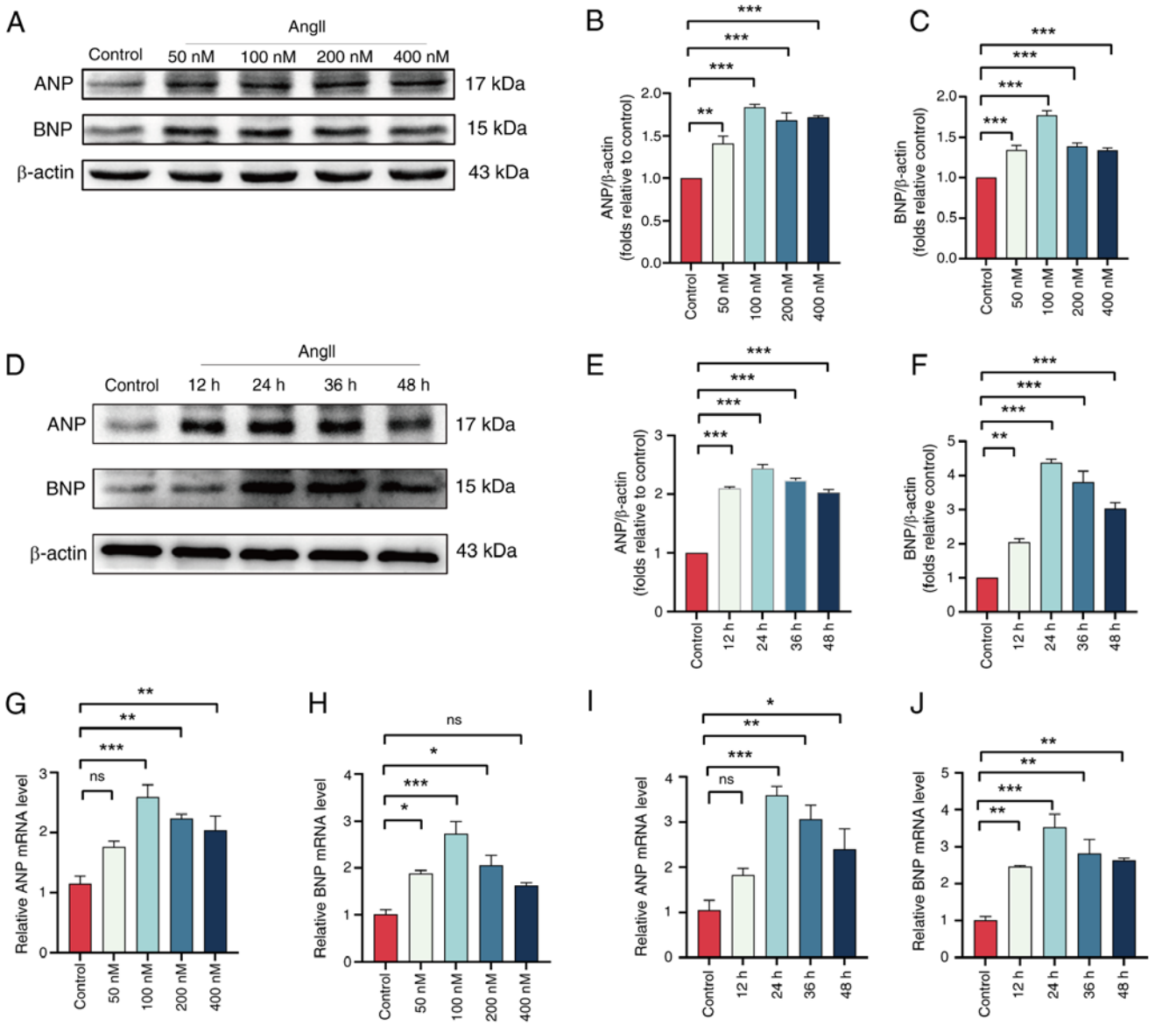

Figure 8. AngII-induced H9c2 cell hypertrophy model. (A-C) Immunoblotting analysis of ANP and BNP protein expression levels in treatment with different concentrations of AngII, along with quantification of the immunoblotting results. β-actin was used as an internal control. (D-F) Immunoblotting analysis of ANP and BNP protein expression levels in treatment with the same concentrations of AngII for different durations, along with quantification of the immunoblotting results. β-actin was used as an internal control. (G and H) Relative mRNA expression levels of (G) ANP and (H) BNP after treatment with different concentrations of AngII. (I and J) Relative mRNA expression levels of (I) ANP and (J) BNP after treatment with the same concentration of AngII for different durations. Error bars represent the SD. Data are presented as the mean ± SD (n=3). *P<0.05, **P<0.01 and ***P<0.001. ns, not significant. AngII, angiotensin II; ANP, atrial natriuretic peptide; BNP, brain natriuretic peptide; ns, not significant.

of tumors (44). MCL1, an anti-apoptotic gene, serves a crucial role in cell survival, metabolism, apoptosis, immunity and tumor formation (47-49). It has attracted attention in research on hematological malignancies (48). Inhibition of MCL1 can promote tumor cell apoptosis and enhance the cytotoxicity or antitumor immune efficacy of drugs in acute myeloid leukemia (AML) (50). Dysregulation or inhibition of MCL1 is an essential factor contributing to drug resistance in various cancer types (51-54), as MCL1 is a major regulatory protein of the intrinsic apoptosis pathway. Given that the PIK3R1/Akt/mTOR signaling pathway is regulated by AT, targeting PIK3R1 can reduce cellular oxidative stress and apoptosis, thereby regulating cardiomyocyte apoptosis in the treatment of heart diseases (55). In addition, PIK3R1 is positively associated with immune activation and serves an essential role in regulating the tumor microenvironment, inflammation and drug sensitivity or resistance (56-59).

CCND1, located on chromosome 11q, is a member of the cell cycle protein D family and serves a crucial role in anti-aging signaling pathways (60). Liu *et al* (61) found that downregulation of CCND1 activated anti-aging signaling pathways, enhanced the expression of antioxidant genes, suppressed the production of reactive oxygen species and prevented the osteogenic differentiation of valve interstitial cells in heart valve disease. CCND1 has been revealed to regulate the viability, proliferation and cell cycle of oral squamous cell carcinoma cells through microRNA-519d-3p (62). Furthermore, detection of CCND1 rearrangements holds

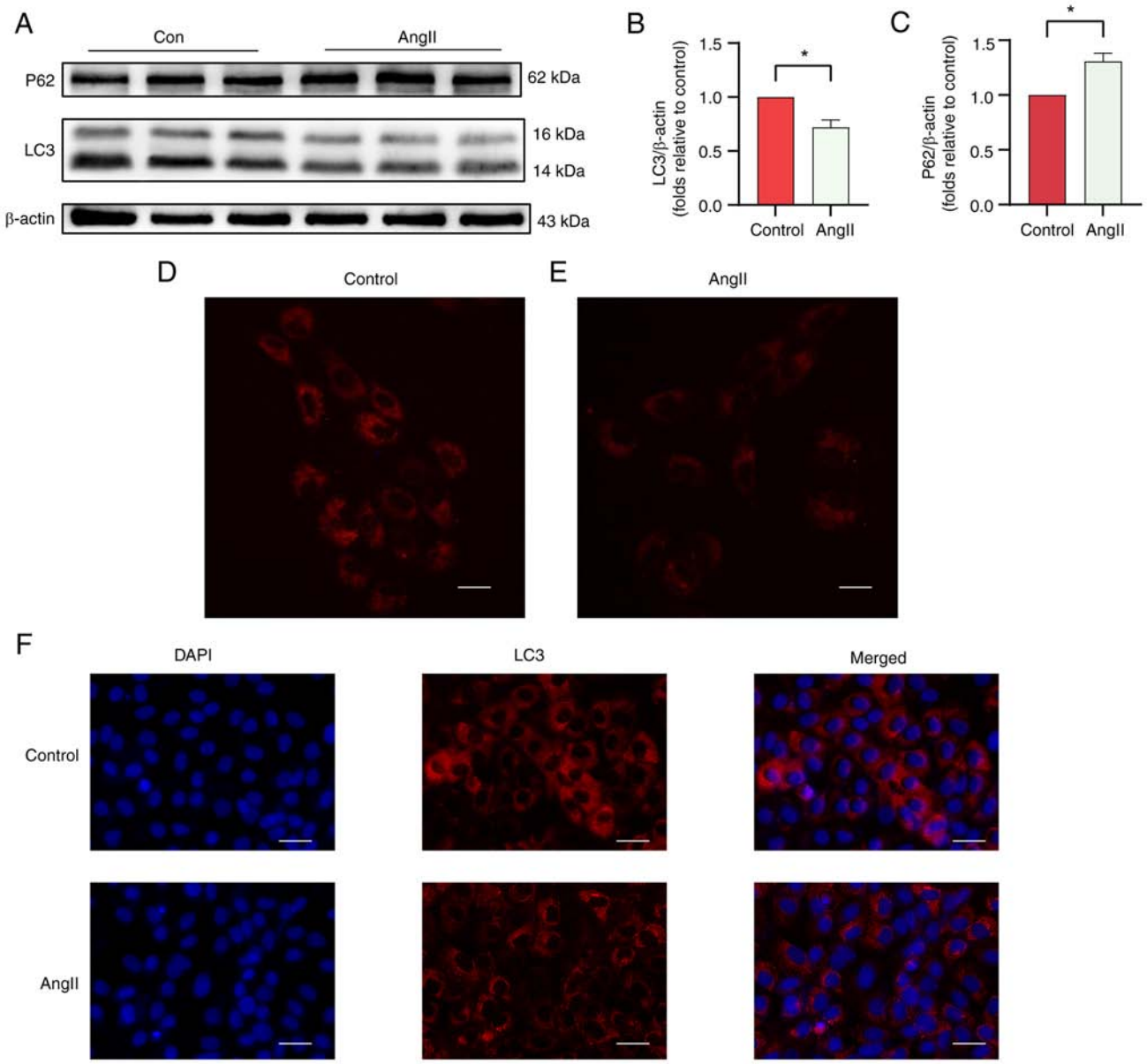

Figure 9. AngII induces changes in the level of autophagy in H9c2 cell hypertrophy. (A) Representative western blotting bands of LC3 and P62. Relative protein expression levels of (B) LC3 and (C) P62, estimated using ImageJ software. (D,E) Lysotracker red fluorescence intensity represented the number of autolysosomes (magnification, x400; scale bar, 100 μm). (F) Representative images of LC3 immunofluorescence in the AngII-induced H9c2 cell hypertrophy model (magnification, x200; scale bar, 50 μm). Error bars represent the SD. Data are presented as the mean ± SD (n=3). *P<0.05. Con, control; AngII, angiotensin II.

diagnostic value for blood disorders (63). PPARG, a member of the peroxisome proliferator-activated receptor subfamily, serves a crucial role in regulating various signaling pathways involved in the pathophysiological mechanisms of various diseases and states, including inflammation, lipid metabolism, AT, apoptosis and cell cycle progression (64,65). Notably, PPARG has been closely associated with chemosensitivity in gastric cancer, AML, colorectal cancer and breast cancer (66), highlighting its important role in modulating the response of tumor cells to chemotherapeutic agents. Mechanistically, PPARG influences chemosensitivity by regulating cell cycle progression and AT, and participating in inflammatory responses (67). In the present study, DSigDB was utilized to predict potential drugs targeting the identified hub genes. The results indicated that rapamycin and Mel are promising drugs targeting ARGs and pathways in HCM. Previous studies have demonstrated the therapeutic efficacy of rapamycin and Melatonin in HCM, which is consistent with the findings of the present study (28,68). However, the therapeutic efficacy of other drugs warrants further investigation and validation.

The precise role of the immune system in the development of HCM remains elusive. Previous studies have demonstrated that AT serves an essential role in immunity, primarily through its involvement in pathogen clearance and inflammation regulation (69-71). Therefore, in the current study, the relationship between ARGs and immune cell infiltration in HCM was investigated. Only the infiltration levels of Tfh cells were significantly different between the HCM and control groups. Tfh cells represent an independent subset of CD4(+) T effector cells involved in humoral immunity and activation of other immune cells (72). The infiltration levels

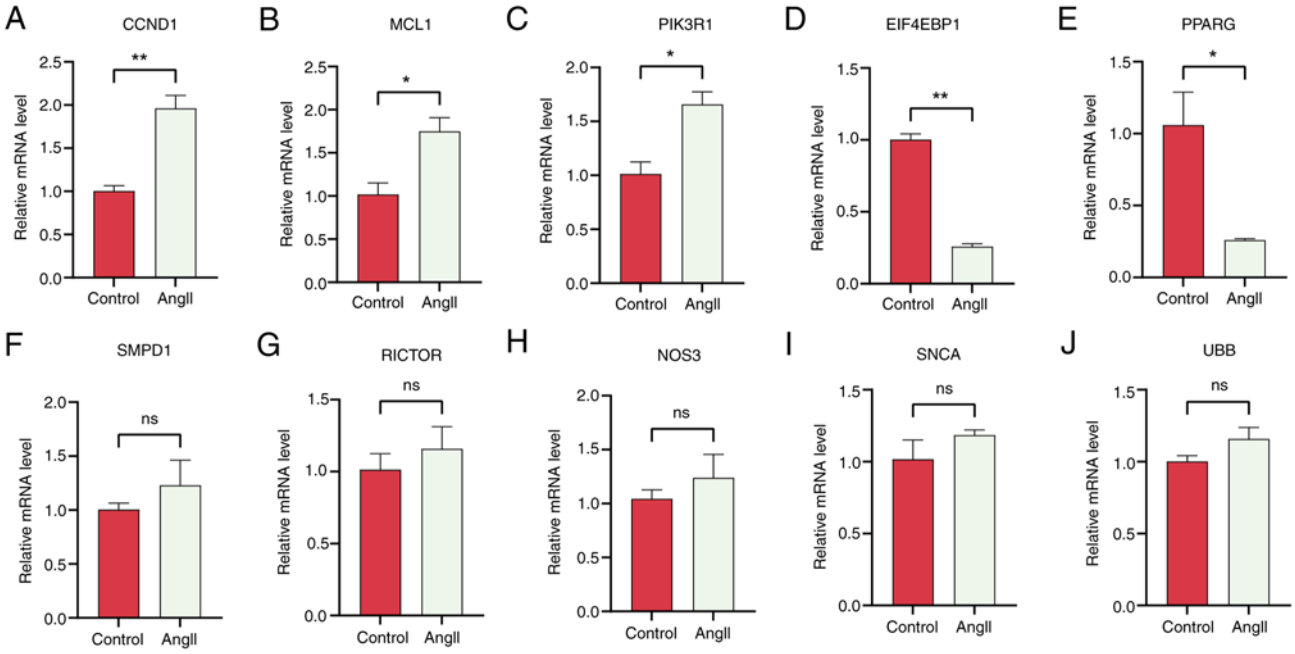

Figure 10. Revalidation of hub genes in AngII-induced H9c2 cell hypertrophy. (A-J) mRNA expression levels of hub genes were detected using reverse transcription-quantitative PCR. Error bars represent the SD. Data are presented as the mean ± SD (n=3). *P<0.05 and **P<0.01. ns, not significant; AngII, angiotensin II.

of Tfh cells were positively correlated with EIF4EBP1 but negatively correlated with MCL1 and PIK3R1. Furthermore, the infiltration levels of monocytes and neutrophils were positively correlated with MCL1, and those of regulatory T cells were negatively correlated with PPARG. However, CCND1 did not exhibit a significant correlation with the 22 immune cell types examined in the present study. These results provided valuable insights into how ARGs influence the development of HCM by regulating immunity. However, the present study did not validate the relationship between immune infiltrating cells and core ARGs through specific experiments. Further research and evidence in this area are required in the future.

The level of autophagic activity reported in studies on HCM is inconsistent possibly due to differences in study participants, experimental design and sample size (73,74). Upregulation of certain ARGs is also observed in HCM, which may be attributed to the following reasons: Firstly, it can be considered as a compensatory mechanism wherein cells attempt to restore autophagic function by increasing the expression of specific ARGs. This upregulation aims to compensate for the reduced autophagic activity either by enhancing particular steps of AT or by augmenting the number of autophagosomes (73,75,76). Secondly, due to the complex nature of HCM as a disease, involving alterations in multiple genes and signaling pathways during its pathological progression, certain factors within this process might contribute to the upregulation of select ARGs (77-79). The objective of the present study was to investigate the function and expression of ARGs in HCM through bioinformatics analysis and cellular experiments in order to predict potential drugs for HCM. A total of 10 drugs targeting hub genes were identified, including rapamycin and Mel. Studies have validated the therapeutic or preventive effects of rapamycin in HCM (26,27,80). Activation of the mTOR signaling pathway serves a crucial role in regulating cell proliferation and protein activation. Rapamycin inhibits mTOR, directly influencing metabolic disorders, fibrosis and myocardial hypertrophy. It attenuates myocardial hypertrophy and fibrosis, while reversing ventricular remodeling and restoring cardiac function (68,73,81,82). Notably, mTOR signaling has been investigated in studies on heart diseases (83). Furthermore, Mel possesses antioxidant properties and exerts protective effects against various cardiovascular diseases, including diabetic cardiomyopathy and myocardial hypertrophy (28,29). Additionally, studies have demonstrated that activation of macrophage stimulating 1/nuclear factor erythroid 2-related factor 2 signaling and MICU1 could effectively reduce oxidative stress, alleviating myocardial hypertrophy (84,85). In addition to rapamycin and Mel, other ARG-targeted drugs predicted in the present study include wortmannin, deguelin, imatinib, everolimus and rosiglitazone. However, the mechanisms of action of these drugs warrant further investigation.

The present study emphasized the important role of AT in HCM. ARGs associated with the development of HCM were analyzed using bioinformatics tools, and the findings were validated using an external dataset and a cell model of HCM. The present study provides novel insights into the pathological mechanisms of HCM and offers promising avenues for developing therapeutic strategies targeting ARGs.

Despite its important findings, the current study had some limitations that should be acknowledged. First, the sample size should be increased to enhance the reliability of the results, and a more comprehensive prospective study is warranted to validate the results of the present study. Second, clinical samples and animal models are required to verify the

functional roles of the identified hub ARGs. Third, validation of the protein expression levels of core ARGs should be added. Lastly, further investigation is required to verify the therapeutic efficacy of the predicted drugs and elucidate the specific mechanisms through which the hub ARGs regulate the development of HCM.

In conclusion, the present study demonstrated that the expression of ARGs was significantly altered in HCM. In particular, EIF4EBP1, MCL1, PIK3R1, CCND1 and PPARG were identified as key ARGs that serve as potential diagnostic markers and therapeutic targets for HCM. Additionally, 10 drugs targeting the key ARGs were identified, which may be used in the ARG-targeted treatment of HCM. In conclusion, the current study improved the understanding of the pathogenesis of HCM and highlighted the potential diagnostic and therapeutic value of ARGs in HCM, providing a crucial theoretical foundation for the development of personalized therapies.

Acknowledgements

Not applicable.

Funding

The present study was supported by the Natural Science Foundation of Jiangxi (grant nos. 20212ACB206011, 20224ACB206002 and 20232BAB206009) and the National Natural Science Foundation of China (grant nos. 82160073 and 81860082).

Availability of data and materials

The data generated in the present study may be requested from the corresponding author.

Authors' contributions

RBQ conducted the cell experiments, and analyzed and mapped the experimental data. STZ contributed to the experimental design and performed data analysis for the bioinformatics analysis. ZWL drafted the article, provided software support and analyzed the data. RYZ, ZCQ, and HZP confirm the authenticity of all the raw data and contributed to data interpretation. LFZ and ZQX contributed to the cell experiments. SQL and LW designed the experiments and provided financial support. All authors read and approved the final version of the manuscript.

Ethics approval and consent to participate

Not applicable.

Patient consent for publication

Not applicable.

Competing interests

The authors declare that they have no competing interests.

References

1. He J, Gu D, Wu X, Reynolds K, Duan X, Yao C, Wang J, Chen CS, Chen J, Wildman RP, *et al*: Major causes of death among men and women in China. N Engl J Med 353: 1124-1134, 2005.
2. Abbas MT, Baba Ali N, Farina JM, Mahmoud AK, Pereyra M, Scalia IG, Kamel MA, Barry T, Lester SJ, Cannan CR, *et al*: Role of genetics in diagnosis and management of hypertrophic cardiomyopathy: A glimpse into the future. Biomedicines 12: 682, 2024.
3. Wang Z, Xia Q, Su W, Cao M, Sun Y, Zhang M, Chen W and Jiang T: Exploring the communal pathogenesis, ferroptosis mechanism, and potential therapeutic targets of dilated cardiomyopathy and hypertrophic cardiomyopathy via a microarray data analysis. Front Cardiovasc Med 9: 824756, 2022.
4. Chase Cole J, Benvie SF and DeLosSantos M: Mavacamten: A novel agent for hypertrophic cardiomyopathy. Clin Ther 46: 368-373, 2024.
5. Zampieri M, Argirò A, Marchi A, Berteotti M, Targetti M, Fornaro A, Tomberli A, Stefàno P, Marchionni N and Olivotto I: Mavacamten, a novel therapeutic strategy for obstructive hypertrophic cardiomyopathy. Curr Cardiol Rep 23: 79, 2021.
6. Ottaviani A, Mansour D, Molinari LV, Galanti K, Mantini C, Khanji MY, Chahal AA, Zimarino M, Renda G, Sciarra L, *et al*: Revisiting diagnosis and treatment of hypertrophic cardiomyopathy: Current practice and novel perspectives. J Clin Med 12: 5710, 2023.
7. Bakalakos A, Monda E and Elliott PM: The diagnostic and therapeutic implications of phenocopies and mimics of hypertrophic cardiomyopathy. Can J Cardiol 40: 754-765, 2024.
8. Pu L, Li J, Qi W, Zhang J, Chen H, Tang Z, Han Y, Wang J and Chen Y: Current perspectives of sudden cardiac death management in hypertrophic cardiomyopathy. Heart Fail Rev 29: 395-404, 2024.
9. Faisaluddin M, Balasubramanian S, Ahmed A, Hussain K, Nso N, Gaznabi S, Erwin JP III, Pursnani A and Ricciardi M: Temporal trends and procedural safety of transcatheter mitral valve repair with mitraclip in patients with hypertrophic cardiomyopathy: Insights from the national inpatient sample. Curr Probl Cardiol 49: 102354, 2024.
10. Yacoub MS, El-Nakhal T, Hasabo EA, Shehata N, Wilson K, Ismail KH, Bakr MS, Mohsen M, Mohamed A, Abdelazim E, *et al*: A systematic review and meta-analysis of the efficacy and safety of Mavacamten therapy in international cohort of 524 patients with hypertrophic cardiomyopathy. Heart Fail Rev 29: 479-496, 2024.
11. Chen X, Tsvetkov AS, Shen HM, Isidoro C, Ktistakis NT, Linkermann A, Koopman WJH, Simon HU, Galluzzi L, Luo S, *et al*: International consensus guidelines for the definition, detection, and interpretation of autophagy-dependent ferroptosis. Autophagy 24: 1213-1246, 2024.
12. Kaplan JL, Rivas VN and Connolly DJ: Advancing treatments for feline hypertrophic cardiomyopathy: The role of animal models and targeted therapeutics. Vet Clin North Am Small Anim Pract 53: 1293-1308, 2023.
13. Rivas VN, Kaplan JL, Kennedy SA, Fitzgerald S, Crofton AE, Farrell A, Grubb L, Jauregui CE, Grigorean G, Choi E, *et al*: Multi-omic, histopathologic, and clinicopathologic effects of once-weekly oral rapamycin in a naturally occurring feline model of hypertrophic cardiomyopathy: A pilot study. Animals (Basel) 13: 3184, 2023.
14. Dang JY, Zhang W, Chu Y, Chen JH, Ji ZL and Feng P: Downregulation of salusins alleviates hypertrophic cardiomyopathy via attenuating oxidative stress and autophagy. Eur J Med Res 29: 109, 2024.
15. Huang X, Zhang J, Wang W, Huang Z and Han P: Vps4a regulates autophagic flux to prevent hypertrophic cardiomyopathy. Int J Mol Sci 24: 10800, 2023.
16. Rabinovich-Nikitin I and Kirshenbaum LA: YAP/TFEB pathway promotes autophagic cell death and hypertrophic cardiomyopathy in lysosomal storage diseases. J Clin Invest 131: e146821, 2021.
17. Zhang Y, Zhao J, Jin Q and Zhuang L: Transcriptomic analyses and experimental validation identified immune-related lncRNA-mRNA Pair MIR210HG-BPIFC regulating the progression of hypertrophic cardiomyopathy. Int J Mol Sci 25: 2816, 2024.
18. Ritchie ME, Phipson B, Wu D, Hu Y, Law CW, Shi W and Smyth GK: limma powers differential expression analyses for RNA-sequencing and microarray studies. Nucleic Acids Res 43: e47, 2015.

19. R Core Team: A Language and Environment for Statistical Computing. R Foundation for Statistical Computing, Vienna, 2020. Available from: https://www.R-project.org/.
20. Chin CH, Chen SH, Wu HH, Ho CW, Ko MT and Lin CY: cytoHubba: Identifying hub objects and sub-networks from complex interactome. BMC Syst Biol 8 (Suppl 4): S11, 2014.
21. Wu T, Hu E, Xu S, Chen M, Guo P, Dai Z, Feng T, Zhou L, Tang W, Zhan L, *et al*: clusterProfiler 4.0: A universal enrichment tool for interpreting omics data. Innovation (Camb) 2: 100141, 2021.
22. Shannon P, Markiel A, Ozier O, Baliga NS, Wang JT, Ramage D, Amin N, Schwikowski B and Ideker T: Cytoscape: A software environment for integrated models of biomolecular interaction networks. Genome Res 13: 2498-2504, 2003.
23. Gong J, Shi B, Yang P, Khan A, Xiong T and Li Z: Unveiling immune infiltration characterizing genes in hypertrophic cardiomyopathy through transcriptomics and bioinformatics. J Inflamm Res 17: 3079-3092, 2024.
24. Li N, Wang W, Zhou H, Wu Q, Duan M, Liu C, Wu H, Deng W, Shen D and Tang Q: Ferritinophagy-mediated ferroptosis is involved in sepsis-induced cardiac injury. Free Radic Biol Med 160: 303-318, 2020.
25. Livak KJ and Schmittgen TD: Analysis of relative gene expres-sion data using real-time quantitative PCR and the 2(-Delta Delta C(T)) method. Methods 25: 402-408, 2001.
26. Gao XM, Wong G, Wang B, Kiriazis H, Moore XL, Su YD, Dart A and Du XJ: Inhibition of mTOR reduces chronic pressure-overload cardiac hypertrophy and fibrosis. J Hypertens 24: 1663-1670, 2006.
27. Völkers M, Konstandin MH, Doroudgar S, Toko H, Quijada P, Din S, Joyo A, Ornelas L, Samse K, Thuerauf DJ, *et al*: Mechanistic target of rapamycin complex 2 protects the heart from ischemic damage. Circulation 128: 2132-2144, 2013.
28. Pei HF, Hou JN, Wei FP, Xue Q, Zhang F, Peng CF, Yang Y, Tian Y, Feng J, Du J, *et al*: Melatonin attenuates postmyocardial infarction injury via increasing Tom70 expression. J Pineal Res 62, 2017.
29. Reiter RJ, Mayo JC, Tan DX, Sainz RM, Alatorre-Jimenez M and Qin L: Melatonin as an antioxidant: Under promises but over delivers. J Pineal Res 61: 253-278, 2016.
30. Dai H, Liu Y, Zhu M, Tao S, Hu C, Luo P, Jiang A and Zhang G: Machine learning and experimental validation of novel biomarkers for hypertrophic cardiomyopathy and cancers. J Cell Mol Med 28: e70034, 2024.
31. Abbasi M, Ong KC, Newman DB, Dearani JA, Schaff HV and Geske JB: Obstruction in hypertrophic cardiomyopathy: Many faces. J Am Soc Echocardiogr 37: 613-625, 2024.
32. McKinney J, Isserow M, Wong J, Isserow S and Moulson N: New insights and recommendations for athletes with hypertrophic cardiomyopathy. Can J Cardiol 40: 921-933, 2024.
33. Schaff HV and Wei X: Contemporary surgical management of hypertrophic cardiomyopathy. Ann Thorac Surg 117: 271-281, 2024.
34. Maron BJ, Rowin EJ and Maron MS: Global burden of hypertrophic cardiomyopathy. JACC Heart Fail 6: 376-378, 2018.
35. Ding X, Zhu C, Wang W, Li M, Ma C and Gao B: SIRT1 is a regulator of autophagy: Implications for the progression and treatment of myocardial ischemia-reperfusion. Pharmacol Res 199: 106957, 2024.
36. Rabinovich-Nikitin I, Kirshenbaum E and Kirshenbaum LA: Autophagy, clock genes, and cardiovascular disease. Can J Cardiol 39: 1772-1780, 2023.
37. Zhao J, Liu GW and Tao C: Hotspots and future trends of autophagy in traditional chinese medicine: A bibliometric analysis. Heliyon 9: e20142, 2023.
38. Sazonova EV, Petrichuk SV, Kopeina GS and Zhivotovsky B: A link between mitotic defects and mitotic catastrophe: Detection and cell fate. Biol Direct 16: 25, 2021.
39. Byrnes K, Blessinger S, Bailey NT, Scaife R, Liu G and Khambu B: Therapeutic regulation of autophagy in hepatic metabolism. Acta Pharm Sin B 12: 33-49, 2022.
40. Xiong R, Li N, Chen L, Wang W, Wang B, Jiang W and Geng Q: STING protects against cardiac dysfunction and remodelling by blocking autophagy. Cell Commun Signal 19: 109, 2021.
41. Ikeda S, Zablocki D and Sadoshima J: The role of autophagy in death of cardiomyocytes. J Mol Cell Cardiol 165: 1-8, 2022.
42. Chen B, Yang Y, Wu J, Song J and Lu J: microRNA-17-5p downregulation inhibits autophagy and myocardial remodelling after myocardial infarction by targeting STAT3. Autoimmunity 55: 43-51, 2022.
43. Zhu QH, Zhou YL, Yang M, Yang BB, Cao WT, Yuan LM and Deng DQ: Reduced miR-99a-3p levels in systemic lupus erythematosus may promote B cell proliferation via NCAPG and the PI3K/AKT signaling pathway. Lupus 33: 365-374, 2024.
44. Voeltzke K, Scharov K, Funk CM, Kahler A, Picard D, Hauffe L, Orth MF, Remke M, Esposito I, Kirchner T, *et al*: EIF4EBP1 is transcriptionally upregulated by MYCN and associates with poor prognosis in neuroblastoma. Cell Death Discov 8: 157, 2022.
45. Wu ZR, Yan L, Liu YT, Cao L, Guo YH, Zhang Y, Yao H, Cai L, Shang HB, Rui WW, *et al*: Inhibition of mTORC1 by lncRNA H19 via disrupting 4E-BP1/Raptor interaction in pituitary tumours. Nat Commun 9: 4624, 2018.
46. Nelson ED, Benesch MG, Wu R, Ishikawa T and Takabe K: High EIF4EBP1 expression reflects mTOR pathway activity and cancer cell proliferation and is a biomarker for poor breast cancer prognosis. Am J Cancer Res 14: 227-242, 2024.
47. Montalban-Bravo G, Thongon N, Rodriguez-Sevilla JJ, Ma F, Ganan-Gomez I, Yang H, Kim YJ, Adema V, Wildeman B, Tanaka T, *et al*: Targeting MCL1-driven anti-apoptotic pathways overcomes blast progression after hypomethylating agent failure in chronic myelomonocytic leukemia. Cell Rep Med 5: 101585, 2024.
48. Mukherjee N, Katsnelson E, Brunetti TM, Michel K, Couts KL, Lambert KA, Robinson WA, McCarter MD, Norris DA, Tobin RP and Shellman YG: MCL1 inhibition targets myeloid derived suppressors cells, promotes antitumor immunity and enhances the efficacy of immune checkpoint blockade. Cell Death Dis 15: 198, 2024.
49. Clerbaux LA, Cordier P, Desboeufs N, Unger K, Leary P, Semere G, Boege Y, Chan LK, Desdouets C, Lopes M and Weber A: Mcl-1 deficiency in murine livers leads to nuclear polyploidisation and mitotic errors: Implications for hepatocellular carcinoma. JHEP Rep 5: 100838, 2023.
50. Chiou JT and Chang LS: Synergistic cytotoxicity of decitabine and YM155 in leukemia cells through upregulation of SLC35F2 and suppression of MCL1 and survivin expression. Apoptosis 29: 503-520, 2024.
51. Boët E and Sarry JE: Targeting metabolic dependencies fueling the TCA cycle to circumvent therapy resistance in acute myeloid leukemia. Cancer Res 84: 950-952, 2024.
52. Mukherjee N, Schwan JV, Fujita M, Norris DA and Shellman YG: Alternative treatments for melanoma: Targeting BCL-2 family members to de-bulk and kill cancer stem cells. J Invest Dermatol 135: 2155-2161, 2015.
53. Kapoor I, Bodo J, Hill BT, Hsi ED and Almasan A: Targeting BCL-2 in B-cell malignancies and overcoming therapeutic resistance. Cell Death Dis 11: 941, 2020.
54. Neophytou CM, Trougakos IP, Erin N and Papageorgis P: Apoptosis deregulation and the development of cancer multi-drug resistance. Cancers (Basel) 13: 4363, 2021.
55. Zhan H, Huang F, Niu Q, Jiao M, Han X, Zhang K, Ma W, Mi S, Guo S and Zhao Z: Downregulation of miR-128 ameliorates Ang II-induced cardiac remodeling via SIRT1/PIK3R1 multiple targets. Oxid Med Cell Longev 2021: 8889195, 2021.
56. Dsouza NR, Cottrell CE, Davies OMT, Tollefson MM, Frieden IJ, Basel D, Urrutia R, Drolet BA and Zimmermann MT: Structural and dynamic analyses of pathogenic variants in PIK3R1 reveal a shared mechanism associated among cancer, undergrowth, and overgrowth syndromes. Life (Basel) 14: 297, 2024.
57. De Bortoli M, Queisser A, Pham VC, Dompmartin A, Helaers R, Boutry S, Claus C, De Roo AK, Hammer F, Brouillard P, *et al*: Somatic loss-of-function PIK3R1 and activating non-hotspot PIK3CA mutations associated with capillary malformation with dilated veins (CMDV). J Invest Dermatol 144: 2066-2077, 2024.
58. Yu X, Xu C, Zou Y, Liu W, Xie Y and Wu C: A prognostic metabolism-related gene signature associated with the tumor immune microenvironment in neuroblastoma. Am J Cancer Res 14: 253-273, 2024.
59. He B, Quan L, Li C, Yan W, Zhang Z, Zhou L, Wei Q, Li Z, Mo J, Zhang Z, *et al*: Targeting ERBB2 and PIK3R1 as a therapeutic strategy for dilated cardiomyopathy: A single-cell sequencing and mendelian randomization analysis. Heliyon 10: e25572, 2024.
60. Maura F and Bergsagel PL: Molecular pathogenesis of multiple myeloma: Clinical implications. Hematol Oncol Clin North Am 38: 267-279, 2024.
61. Liu Z, Wang K, Jiang C, Chen Y, Liu F, Xie M, Yim WY, Yao D, Qian X, Chen S, *et al*: Morusin alleviates aortic valve calcification by inhibiting valve interstitial cell senescence through Ccnd1/Trim25/Nrf2 axis. Adv Sci (Weinh) 19: e2307319, 2024.

62. Zhang W and Hong W: Upregulation of miR-519d-3p inhibits viability, proliferation, and G1/S cell cycle transition of oral squamous cell carcinoma cells through targeting CCND1. Cancer Biother Radiopharm 39: 153-163, 2024.
63. Quesada AE, Hu S, Li S, Toruner GA, Wei Q, Loghavi S, Ok CY, Jain P, Thakral B, Nwogbo OV, *et al*: Optical genomic mapping is a helpful tool for detecting CCND1 rearrangements in CD5-negative small B-cell lymphoma: Two cases of leukemic non-nodal mantle cell lymphoma. Hum Pathol 144: 71-76, 2024.
64. Han B, Chen J, Chen S, Shen X, Hou L, Fang J and Lian M: PPARG and the PTEN-PI3K/AKT signaling axis may cofunction in promoting chemosensitivity in hypopharyngeal squamous cell carcinoma. PPAR Res 2024: 2271214, 2024.
65. Qin Y, Ashrafizadeh M, Mongiardini V, Grimaldi B, Crea F, Rietdorf K, Győrffy B, Klionsky DJ, Ren J, Zhang W and Zhang X: Autophagy and cancer drug resistance in dialogue: Pre-clinical and clinical evidence. Cancer Lett 570: 216307, 2023.
66. Jia Q, Li B, Wang X, Ma Y and Li G: Comprehensive analysis of peroxisome proliferator-activated receptors to predict the drug resistance, immune microenvironment, and prognosis in stomach adenocarcinomas. PeerJ 12: e17082, 2024.
67. Sun Y, Ma J, Lin J, Sun D, Song P, Shi L, Li H, Wang R, Wang Z and Liu S: Circular RNA circ_ASAP2 regulates drug sensitivity and functional behaviors of cisplatin-resistant gastric cancer cells by the miR-330-3p/NT5E axis. Anticancer Drugs 32: 950-961, 2021.
68. Choi JC, Muchir A, Wu W, Iwata S, Homma S, Morrow JP and Worman HJ: Temsirolimus activates autophagy and ameliorates cardiomyopathy caused by lamin A/C gene mutation. Sci Transl Med 4: 144ra102, 2012.
69. Gan T, Qu S, Zhang H and Zhou XJ: Modulation of the immunity and inflammation by autophagy. MedComm (2020) 4: e311, 2023.
70. Herb M, Gluschko A and Schramm M: LC3-associated phagocytosis-the highway to hell for phagocytosed microbes. Semin Cell Dev Biol 101: 68-76, 2020.
71. Castillo EF, Dekonenko A, Arko-Mensah J, Mandell MA, Dupont N, Jiang S, Delgado-Vargas M, Timmins GS, Bhattacharya D, Yang H, *et al*: Autophagy protects against active tuberculosis by suppressing bacterial burden and inflammation. Proc Natl Acad Sci USA 109: E3168-E3176, 2012.
72. Ma CS: Human T follicular helper cells in primary immunodeficiency: Quality just as important as quantity. J Clin Immunol 36 (Suppl 1): S40-S47, 2016.
73. Singh SR, Zech ATL, Geertz B, Reischmann-Düsener S, Osinska H, Prondzynski M, Krämer E, Meng Q, Redwood C, van der Velden J, *et al*: Activation of autophagy ameliorates cardiomyopathy in mybpc3-targeted knockin mice. Circ Heart Fail 10: e004140, 2017.
74. Hassoun R, Budde H, Zhazykbayeva S, Herwig M, Sieme M, Delalat S, Mostafi N, Gömöri K, Tangos M, Jarkas M, *et al*: Stress activated signalling impaired protein quality control pathways in human hypertrophic cardiomyopathy. Int J Cardiol 344: 160-169, 2021.
75. Simpson JE and Gammoh N: Autophagy cooperates with PDGFRA to support oncogenic growth signaling. Autophagy 20: 1901-1902, 2024.
76. Ravikumar B, Sarkar S, Davies JE, Futter M, Garcia-Arencibia M, Green-Thompson ZW, Jimenez-Sanchez M, Korolchuk VI, Lichtenberg M, Luo S, *et al*: Regulation of Mammalian autophagy in physiology and pathophysiology. Physiol Rev 90: 1383-1435, 2010.
77. Marian AJ and Braunwald E: Hypertrophic cardiomyopathy: Genetics, pathogenesis, clinical manifestations, diagnosis, and therapy. Circ Res 121: 749-770, 2017.
78. Tannous P, Zhu H, Johnstone JL, Shelton JM, Rajasekaran NS, Benjamin IJ, Nguyen L, Gerard RD, Levine B, Rothermel BA and Hill JA: Autophagy is an adaptive response in desmin-related cardiomyopathy. Proc Natl Acad Sci USA 105: 9745-9750, 2008.
79. Sheng SY, Li JM, Hu XY and Wang Y: Regulated cell death pathways in cardiomyopathy. Acta Pharmacol Sin 44: 1521-1535, 2023.
80. Buss SJ, Muenz S, Riffel JH, Malekar P, Hagenmueller M, Weiss CS, Bea F, Bekeredjian R, Schinke-Braun M, Izumo S, *et al*: Beneficial effects of Mammalian target of rapamycin inhibition on left ventricular remodeling after myocardial infarction. J Am Coll Cardiol 54: 2435-2446, 2009.
81. Sciarretta S, Volpe M and Sadoshima J: Mammalian target of rapamycin signaling in cardiac physiology and disease. Circ Res 114: 549-564, 2014.
82. Marin TM, Keith K, Davies B, Conner DA, Guha P, Kalaitzidis D, Wu X, Lauriol J, Wang B, Bauer M, *et al*: Rapamycin reverses hypertrophic cardiomyopathy in a mouse model of LEOPARD syndrome-associated PTPN11 mutation. J Clin Invest 121: 1026-1043, 2011.
83. Sciarretta S, Forte M, Frati G and Sadoshima J: New insights into the role of mTOR signaling in the cardiovascular system. Circ Res 122: 489-505, 2018.
84. Yang Y, Du J, Xu R, Shen Y, Yang D, Li D, Hu H, Pei H and Yang Y: Melatonin alleviates angiotensin-II-induced cardiac hypertrophy via activating MICU1 pathway. Aging (Albany NY) 13: 493-515, 2020.
85. Chen S, Sun P, Li Y, Shen W, Wang C, Zhao P, Cui H, Xue JY and Du GQ: Melatonin activates the Mst1-Nrf2 signaling to alleviate cardiac hypertrophy in pulmonary arterial hypertension. Eur J Pharmacol 933: 175262, 2022.